Accelerative propagation and explosion triggering by expanding turbulent premixed flames

V'yacheslav Akkerman*
Department of Mechanical and Aerospace Engineering, West Virginia University, Morgantown, West Virginia 26506-6106, USA

Swetaprovo Chaudhuri and Chung K. Law
Department of Mechanical and Aerospace Engineering, Princeton University, Princeton, New Jersey 08544-5263, USA

(Received 13 July 2012; revised manuscript received 24 September 2012; published 13 February 2013)

The dynamics and morphology of outwardly propagating, accelerating turbulent premixed flames and the effect of flame acceleration on explosion triggering are analyzed. Guided by recent theoretical results and substantiated by experiments, we find that an expanding flame front in an externally forced, near-isotropic turbulent environment exhibits accelerative propagation given by a well-defined power law based on the average global flame radius. In this context the limits of the power-law exponent and the effective turbulence intensity experienced by the flame are derived. The power-law exponent is found to be substantially larger than that for the hydrodynamically unstable cellular laminar flames, hence facilitating the possibility of detonation triggering in turbulent environments. For large length scales, hydrodynamic instability is expected to provide additional acceleration, thus further favoring the attainment of detonation triggering.

DOI: 10.1103/PhysRevE.87.023008 PACS number(s): 47.70.Pq, 47.27.−i, 47.15.−x, 47.40.−x

I. INTRODUCTION

Turbulent burning rate is a key parameter in the study of turbulent combustion, as emphasized in the representative experimental [1,2], computational [3] and analytical [4–6] studies. In particular, there exists considerable interest to identify, at least for a certain special class of flows such as isotropic turbulence, a unified functional description of the premixed turbulent flame speed, S_T,

$$S_T = f(U_{\rm rms}, \lambda_I, \ldots S_L, \delta_L, \ldots), \tag{1}$$

in which the turbulent root-mean-square (rms) velocity, $U_{\rm rms}$, also known as the turbulence intensity, and the integral turbulence length scale, λ_I, characterize the turbulent flow, while the unstretched laminar flame speed, S_L, and the thermal flame thickness, δ_L—estimated conventionally as $\delta_L \equiv D_{th}/S_L$, where D_{th} is the thermal diffusivity of the fresh gas—describe the flame dynamics. Then, in the limit of moderate to large Damköhler number, turbulent flame propagation can be reduced to a geometric problem, as turbulence corrugates the flame front at a multitude of length scales without perturbing the inner flame structure. Consequently, based on scaling considerations, the quantity S_T can be expressed as

$$S_T/S_L = f(U_{\rm rms}/S_L, \lambda_I/\delta_L). \tag{2}$$

Furthermore, it has been proposed [7] that the scaled velocity and length parameters in Eq. (2), $U_{\rm rms}/S_L$ and λ_I/δ_L, can be collapsed to a single parameter, a turbulence Reynolds number $\mathrm{Re}_{T,M}$, such that

$$S_T/S_L = f(\mathrm{Re}_{T,M}), \quad \mathrm{Re}_{T,M} = (U_{\rm rms}/S_L)(\lambda_I/\delta_M), \tag{3}$$

where δ_M is the Markstein length, $\delta_M = \mathrm{Mk}\delta_L$, with the Markstein number Mk. Based on Eq. (3), for unity Lewis number flames, Le = 1, with constant Mk, Chaudhuri *et al.* [7] further developed the relation

$$S_T/S_L = C_1 \mathrm{Re}_{T,M}^{1/2}, \tag{4}$$

with the phenomenological constant C_1 being order of unity. Since $\delta_M = \mathrm{Mk}\delta_L$, for a constant Mk, i.e., for a given mixture, one can also write

$$S_T/S_L = C_1 \mathrm{Re}_T^{1/2}, \quad \mathrm{Re}_T = (U_{\rm rms}/S_L)(\lambda_I/\delta_L). \tag{5}$$

In this paper we do not consider Le effect, and it is noted that the result (5) for unity Le, constant but positive Mk is exactly same as that derived by Damkohler [4] and Peters [6] in the limit of small scale turbulence.

The above formulation considers the turbulence intensity and integral length scale in Eq. (3) as independent quantities, although for any given turbulence spectrum the local effect of turbulence on a flame front depends on the largest length scale related to the flame, λ_f, and is described by a certain "effective" turbulent intensity, $u'_{\rm eff} = u'_{\rm eff}(\lambda_f)$, with $U_{\rm rms} = u'_{\rm eff}(\lambda_I)$. In addition, the analysis does not differentiate between the reference turbulence quantities and those related to flame propagation, while in reality the local turbulence intensity "experienced" by the flame differs from the real intensity of the turbulent flow at the flame scale [8], and the characteristic hydrodynamic scale of the flame front can differ from the velocity integral length scale determined by the characteristic size of the combustion chamber or the tools used in generating turbulence, such as grids, fans, etc. To address these issues, in the present work we consider that the flame-related turbulence Reynolds number,

$$\mathrm{Re}_{T,f} = (u'_{\rm eff}/S_L)(\lambda_f/\delta_M), \tag{6}$$

accounts for the relation between the flame-related integral length λ_f and the respective flame-related counterpart of turbulence intensity. The formulation is illustrated based on the classical Obukhov-Kolmogorov spectrum, but can be extended to any given spectrum.

The difference between Eqs. (3) and (6) is of primary importance for expanding flames, whose length scale is characterized

*Vyacheslav.Akkerman@mail.wvu.edu
Phone: +1.304.293.0802 Fax: +1.304.293.6689

by the instantaneous global (or global-in-mean) flame radius, growing in time, while the velocity integral turbulence length scale is fixed. Consequently, the corresponding extension of Eq. (3),

$$S_T/S_L = f(\mathrm{Re}_{T,f}), \tag{7}$$

with $\mathrm{Re}_{T,f}$ given by Eq. (6), predicts a noticeable increase in S_T with the global-in-mean flame radius. It is noted that such strong flame acceleration was also observed in the computational studies of Fru *et al.* [9] and experimental measurements of Lawes *et al.* [10], and it is also substantiated by our recent experiments [11] involving expanding turbulent flames in constant-pressure, near-isotropic turbulence. As a result, in this paper we demonstrate the self-similar-in-mean propagation of an expanding turbulent flame front, with the evolution of the global-in-mean flame radius in the form $\propto t^3$ to the leading order for large t, which strongly exceeds the respective power dependence for an expanding laminar flame corrugated by the hydrodynamic, Darrieus-Landau (DL) flame instability [12]. In this light we also mention in passing a concomitant, Lipatnikov-Chomiak formulation on expanding turbulent flames, based on the concept of turbulent Markstein length [13].

While the majority of the turbulent flame theories do not consider the effect of thermal expansion in the burning process, and as such assume that the flame front is hydrodynamically stable and it does not influence the external turbulent flow, the thermal expansion factor is typically as large as $\Theta \equiv \rho_u/\rho_b = 5 \sim 10$ such that the flame front not only substantially modifies the turbulent flow but it is also subjected to the DL instability [14]. Only a few theoretical analyses have accounted for both turbulence and DL instability [7,15–23]. In particular, the analysis of Chaudhuri *et al.* [7] examined the effects of turbulence on the development of flame front instability based on the hypothesis of the separation of the DL instability and turbulence time scales, estimating whether the instability can develop in the presence of turbulence of given intensity and integral length scale. An expression was then proposed for the turbulent flame speed based on the concept of an effective laminar flame with an effective DL cutoff, superposed on the turbulent flame speed with zero thermal expansion.

We then incorporate the DL effects into the analysis of expanding turbulent flames, predicting further amplification of the flame acceleration due to the DL instability. Following the self-similar formulations of Taylor [24] and Akkerman *et al.* [25], we consider an expanding flame front, corrugated by the DL instability as well as turbulence, as a quasi-one-dimensional-in-mean front propagating into the fresh gas. We shall determine the evolution of the velocity and temperature profiles ahead of the flame and the gas compressibility, as well as the instant and locus of detonation triggering by the accelerating flame front.

II. TURBULENT FLAME FORMULATION

First, we briefly consider the relations between a wave number k of the turbulence perturbation of length scale $\lambda = 2\pi/k$, the local counterpart of the turbulent kinetic energy $\mathrm{K}(k)$, and the turbulence Reynolds number Re_T. For the conventional, Kolmogorov spectrum [26], we have the turbulent energy spectral density $\omega(k) \propto k^{-5/3}$, so $\mathrm{K}(k)$ is given by

$$\mathrm{K}(k) = \int_k^{k_K} \omega(\tilde{k})d\tilde{k} \cong k^{-2/3} \propto \lambda^{2/3}, \tag{8}$$

with $(U_{\mathrm{rms}})^2 = \mathrm{K}(k_I) \propto (\lambda_I)^{2/3}$ and $(u'_{\mathrm{eff}})^2 = \mathrm{K}(k_f) \propto (\lambda_f)^{2/3}$. Here $k_I = 2\pi/\lambda_I$ is the integral turbulence wave number, $k_f = 2\pi/\lambda_f$ and $k_K = 2\pi/\lambda_K$ is the Kolmogorov wave number, with $k_K \gg k > k_I$, $\lambda_I > \lambda \gg \lambda_K$. It is noted that the expression for u'_{eff} above is not a conventional turbulent root-mean-square velocity defined in the turbulence literature, where the averaging is performed over the entire ensemble. In contrast, here the averaging is performed over a domain size equal to the respective flame size such that the effective fluctuating velocity experienced by the flame front could be estimated. It is suggested that any eddy of the length scale exceeding the flame size convects the entire flame rather than inducing flame surface fluctuations that are of interest here. Formally, one can also consider a quantity

$$u''^{\,2}_{\mathrm{eff}} = \frac{1}{N}\sum_{i=1}^{N}[u_r - \langle u_r\rangle_R]^2, \tag{9}$$

where u_r is the radial component of the local velocity and $\langle u_r\rangle_R$ is the averaging of an instantaneous, one-time probability density function (pdf) realization of u_r over a domain of size R. However, being always positive but a fluctuating quantity, u''_{eff} can therefore be ensemble-averaged (say, in time) to yield $u'_{\mathrm{eff}} = \langle u''_{\mathrm{eff}}\rangle$.

It is also noted that while Eq. (8) is obtained with the approach of isotropic, Kolmogorov turbulence, the formulation can be extended to an arbitrary spectrum. For instance, with the Pope spectrum [27],

$$\omega(k) \propto k^{-5/3} f_I(k\lambda_I) f_K(k\lambda_K), \tag{10}$$

where the function $f_I(x)$ provides the shape of the energy-containing range, tending to unity for large x, and the function $f_K(x)$ determines the shape of the dissipation range, tending to unity for small x,

$$f_I(x) \sim \left(\frac{x}{\sqrt{x^2 + b_1^2}}\right)^{11/3},$$
$$f_K(x) \sim \exp\left(-b_2\left\{\sqrt[4]{x^4 + b_3^4} - b_3\right\}\right),$$
$$b_1, b_2, b_3 = \mathrm{const}, \tag{11}$$

we would obtain a lower scale dependence as compared to Eq. (8). Figure 1 shows the evolution of the scaled turbulent flame speed and the average global flame radius in experiments [11] for CH_4-air flames. According to these measurements, we fit $u'_{\mathrm{eff}}(\langle R\rangle) \sim \langle R\rangle^{0.233}$, Fig. 1(a), which agrees with Eq. (8) reasonably well.

We next analyze the limitations on the scale dependence of the turbulent flame speed. Figure 2 shows the experimental snapshot of the "mean spherical turbulent flame brush" held between the global inner, R_{in}, and outer, R_{out}, flame radii [11]. Assuming that the width of such a brush h_T, which is a measure of the largest flame corrugation length scale, is proportional to the global flame radius R_f, $h_T \propto R_f$; with $R_{\mathrm{in}} = R_f - h_T/2$, $R_{\mathrm{out}} = R_f + h_T/2$, we estimate the entire

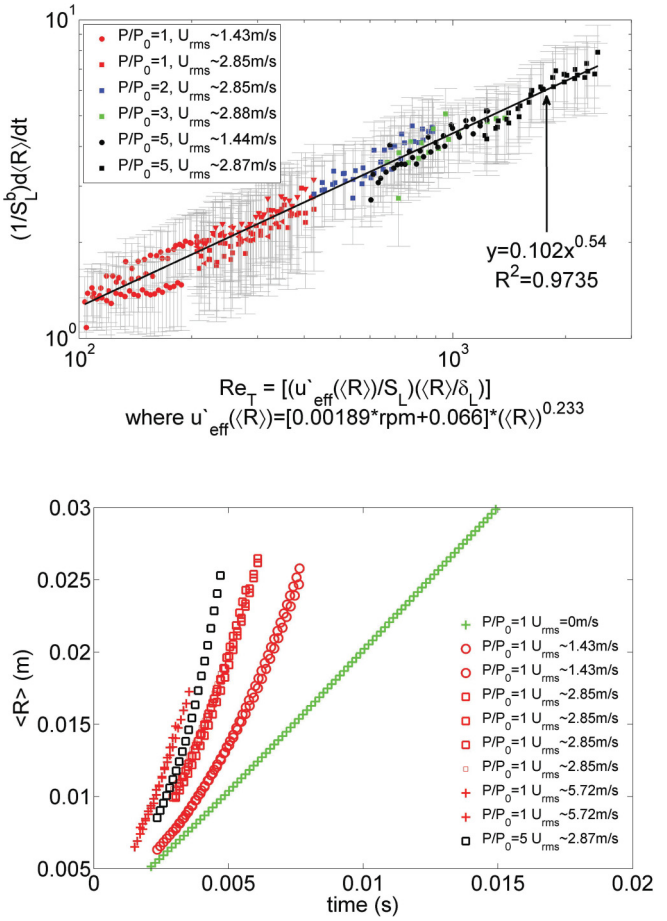

FIG. 1. (Color online) Scaled turbulent flame speed versus the turbulent Reynolds number (a) and the average global flame radius versus time (b) for CH_4-air $\phi = 0.9$ flames in experiments of Ref. [11].

volume of the flame-brush region, i.e., the layer between the inner and outer spheres, as

$$V_T = \frac{4}{3}\pi\left(R_{\text{out}}^3 - R_{\text{in}}^3\right) = 4\pi h_T\left(R_f^2 + h_T^2/12\right) \approx 4\pi h_T R_f^2 \propto R_f^3. \quad (12)$$

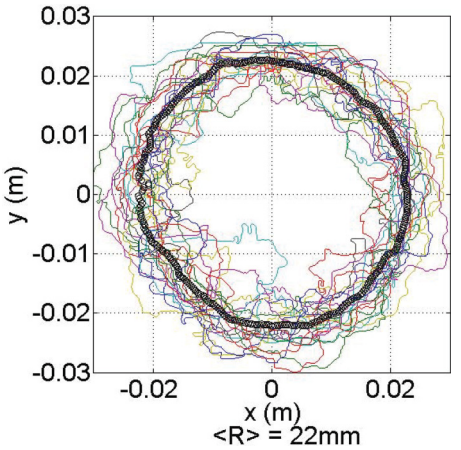

FIG. 2. (Color online) Experimental snapshot of the mean spherical turbulent flame brush [11].

Consequently, the maximum flame-front surface area that can be packed into such a layer is $A_{T,\max} \sim V_T/\delta_L \propto R_f^3$. Within the geometrical consideration of the turbulent flame front, its propagation speed is proportional to the real corrugated flame-front surface area scaled by the area of a hypothetical smooth front of the same radius, $S_T/S_L \propto A_T/4\pi R_f^2$, which cannot exceed the maximum value above, $A_T \leqslant A_{T,\max}$. As a result, the maximum possible turbulent flame speed, $S_{T,\max} = S_T(A_{T,\max})$, would behave as $S_{T,\max} \propto R_f$ such that the radius dependence of the real turbulent flame speed, $S_T(R_f)$, cannot be stronger than the linear one.

We can also arrive at the same conclusion based on the self-similar formulation. Indeed, assuming self-similar flame acceleration in the form $R_f \propto t^\beta$, we find $S_T \propto dR_f/dt \propto t^{\beta-1} \propto R_f^\chi$, with $\chi \equiv (\beta - 1)/\beta$. Obviously, the flame front accelerates only if $\beta > 1$, i.e., $\chi < 1$.

We therefore conclude that the evolution of the turbulent flame speed does not exceed a first-power dependence on the flame radius, which agrees with the theoretical predictions [7] and experimental observations [11] through Eqs. (6) and (8):

$$S_T < S_{T,\max} \propto R_f^1 \propto \text{Re}_{T,f}^{3/4}. \quad (13)$$

Extrapolating the theory of statistically planar premixed flames in isotropic turbulent environment [7] to expanding turbulent flames, we choose the flame integral length scale to be proportional to the flame hydrodynamic length scale $\lambda_f \sim R_f$, as illustrated in Fig. 3, with $\text{Re}_{T,f} = (u'_{\text{eff}}(R_f)/S_L)(R_f/\delta_M)$. Subsequently, Eq. (7) acquires the form

$$\frac{S_T}{S_L} = C_1\text{Re}_{T,f}^{1/2} = C_1\left[\frac{u'_{\text{eff}}(\lambda_I)}{S_L}\left(\frac{R_f}{\lambda_I}\right)^{1/3}\frac{R_f}{\delta_M}\right]^{1/2} = C_1\left(\frac{U_{\text{rms}}}{S_L}\right)^{1/2}\frac{R_f^{2/3}}{\lambda_I^{1/6}\delta_M^{1/2}}. \quad (14)$$

On the other hand, the turbulent flame speed near the unburnt gas locus, say, at a mean progress variable $\langle c\rangle \sim 0.05$, is related to the global-in-mean flame radius as

$$\tilde{c}\Theta S_T = dR_f/dt, \quad (15)$$

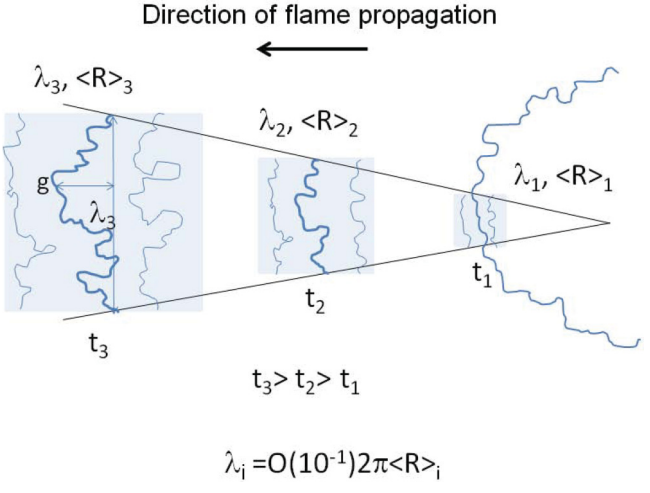

FIG. 3. (Color online) Illustration of the statistically quasi planar assumption for an expanding flame to utilize the theoretical scaling of Ref. [7].

where $\tilde{c}$ is the proportionality coefficient of the order of unity. With Eq. (15), the 2/3 power dependence of Eq. (14) can be integrated as

$$R_f = \left\{R_0^{1/3} + C_2^{1/3}(t - t_0)\right\}^3, \tag{16}$$

where

$$C_2 = \left(\frac{\tilde{c}C_1\Theta}{3}\right)^3 \frac{(U_{\rm rms}S_L)^{3/2}}{\lambda_I^{1/2}\delta_M^{3/2}}, \tag{17}$$

which yields

$$R_f = C_2 t^3 \tag{18}$$

to the leading order for large t, $t \gg t_0$. The parameters t_0 and $R_0 = R_f(t_0)$ denote the instant and locus when the expanding flame front achieves the self-similar-in-mean mode of propagation. Based on dimensional analysis, we estimate $t_0 \sim \lambda_I/U_{\rm rms}$. It is noted that the latter quantity was large enough in the conditions of experiments [11], being of the order of the entire time scale of the problem, which could clearly elucidate why the experimental measurements of Ref. [11] agree very well with the 2/3 power dependence of Eq. (14), see Fig. 1(a), but they do not reproduce the cubic law (18) so well; see Fig. 1(b).

It is recalled that the cubic dependence of Eq. (18) shows much stronger flame acceleration than that for the freely propagating laminar flames with the suggested acceleration exponent α being reported to fall in the range $\alpha = 1.25 - 1.5$ [12,28–30]. This result therefore predicts a much earlier transition to detonation in the present turbulent environment than that in a quiescent laminar one; see Sec. IV.

Here we elucidate the conceptual difference between the recent work of Gostintsev *et al.* [29] and the present formulation, with much stronger flame acceleration in the latter than that in the former. The essential point to note is that the two studies are concerned with two completely different physical situations; namely, the study of Ref. [29] is devoted to a *quiescent* environment, with the vortical motion generated through inherent flame-front cellular instability, while in the present work turbulence is *imposed*, which in addition also allows for the flame-generated vorticity. The imposition of turbulence imitates the fan-generated turbulence in the experiments of Ref. [11]. Consequently, with Eq. (4) for the flame speed in imposed turbulence, we arrive at more powerful acceleration, Eqs. (16) and (18), than that in Ref. [29].

III. TURBULENT FLAMES FURTHER CORRUGATED BY HYDRODYNAMIC INSTABILITY

Although the expansion ratio is included in Eq. (18), the analysis of Sec. II does not incorporate indirect effects of thermal expansion such as the DL instability, which can strongly contribute to the flame acceleration, especially at large scales. Specifically, it is noted that while an embryonic spherical flame front is smooth, being stabilized by stretch, as soon as the flame thickness as compared to the global flame radius is reduced, the generation of the DL instability is favored, leading to the cell formation over the flame surface. Subsequently, the continuous production of new cascades of cells is accompanied by the corresponding continuous increase in the total flame surface area as compared to the globally spherical flame front. It is recalled that, in the absence of turbulence, extensive experimental [12,26,28] and computational [31–34] studies yield the evolution of the globally spherical front described by a power law,

$$R_f \approx B\, t^\alpha, \tag{19}$$

where $\alpha = 1.25 - 1.5$ [12,28–30] and the coefficient B can be estimated as [25,31]

$$B = k_c^{\alpha-1}(\tilde{c}\Theta S_L/\alpha)^\alpha, \tag{20}$$

with $S_{\rm DL}(R_f)/S_L = (k_c R_f)^{(\alpha-1)/\alpha}$, where $k_c \equiv 2\pi/\lambda_c$ is the DL cutoff wave number [14]. Our next step is to incorporate the DL instability into the analysis of expanding turbulent flames in Sec. II.

In Ref. [7], the effects of turbulence on the development of flame-front instability were estimated based on the hypothesis of separation of the DL instability and turbulence time scales. Specifically, we introduced the concept of an effective laminar flame with an effective, turbulence-induced DL cutoff λ_T given by

$$\lambda_T = 4\lambda_c\left[\frac{u'_{\rm eff}(\lambda_c)}{(3/4){\rm X}(\Theta)S_L}\right]^3, \tag{21}$$

$${\rm X}(\Theta) = \frac{\Theta}{\Theta+1}[(\Theta + 1 - \Theta^{-1})^{1/2} - 1]. \tag{22}$$

Then an expression for the turbulent flame speed, based on the effective laminar flame speed superposed on the turbulent flame speed with zero thermal expansion, was proposed; see Ref. [7] for further details and justification. Following the same approach, here we replace Eq. (20) by its turbulence counterpart,

$$B_T = k_T^{\alpha-1}(\tilde{c}\Theta S_T/\alpha)^\alpha, \tag{23}$$

with S_T and $k_T = 2\pi/\lambda_T$ determined by Eqs. (14) and (21), respectively. We subsequently arrive at the final, modified power law,

$$R_f = C_3 t^{3\alpha}, \tag{24}$$

$$C_3 = \left(\frac{27\pi{\rm X}^3}{8}\right)^{\alpha-1}\left(\frac{S_L}{U_{\rm rms}}\right)^{3(\alpha-1)}\left[\frac{3\tilde{c}^3\Theta^3C_1^3}{27\alpha}\frac{(U_{\rm rms}S_L)^{3/2}}{\lambda_I^{1/2}\delta_M^{3/2}}\right]^\alpha \times \frac{\lambda_I^{\alpha-1}}{\lambda_c^{2(\alpha-1)}}, \tag{25}$$

which shows much stronger flame acceleration as compared to the laminar case, Eq. (19). For instance, with $\alpha = 4/3$, Eqs. (19) and (24) yield $R_f \propto t^{4/3}$ and $R_f \propto t^4$, respectively. It is noted that in the limit of no DL instability, $\alpha = 1$, Eq. (24) reduces to Eq. (18), thereby substantiating the self-consistency of the present theory. However, with $U_{\rm rms} = 0$, Eq. (24) does not degenerate to the laminar result (19) because Eqs. (14) and (21) are based on the assumption of strong turbulence, at least $U_{\rm rms} > S_L$.

IV. FLAME-GENERATED FLOW AND EXPLOSION TRIGGERING

We next investigate the possibility of explosion triggering by an outwardly expanding, accelerating turbulent flame front. A similar problem was solved by Taylor [24], who analyzed

the situation of a spherical piston expanding with a constant speed, when the upstream, spherically symmetric equations of continuity and motion,

$$\frac{\partial\rho}{\partial t}+\frac{\partial}{\partial r}(\rho u)+2\rho\frac{u}{r}=0, \tag{26}$$

$$\frac{\partial u}{\partial t}+u\frac{\partial u}{\partial r}+\frac{1}{\rho}\frac{\partial P}{\partial r}=0, \tag{27}$$

acquire a scale-invariant form. The formulation of Ref. [24] was recently extended to an accelerating front allowing for mass passing through it [25].

Unlike Ref. [25], here we consider a turbulent environment instead of a quiescent one, which means that the Reynolds-averaged quantities should be incorporated into the formulation instead of the instantaneous ones. Subsequently, while the continuity equation (26) does not change its form after the Reynolds averaging, the counterpart of the Euler equation (27), in the general form, reads

$$\frac{\partial\langle u_j\rangle}{\partial t}+\langle u_i\rangle\frac{\partial\langle u_j\rangle}{\partial x_i}+\frac{1}{\rho}\frac{\partial}{\partial x_j}\left\{\langle P_{ii}\rangle+\frac{1}{3}\rho U_{\rm rms}^2\delta_{ij}+a_{ij}\right\}=0, \tag{28}$$

where δ_{ij} is the Kronecker operator and a_{ij} is the anisotropy tensor. However, to make our formulation self-consistent, we assume turbulence to be isotropic, $a_{ij}=0$, and unaffected by flame propagation, $\partial(U_{\rm rms}^2\delta_{ij})/\partial x_j=0$. Consequently, Eq. (28) acquires the form identical to Eq. (27), and the subsequent formulation resembles that of Ref. [25] for the laminar environment.

Following the same approach, we transform the variables (r,t) to (η,τ), with $\eta\equiv r/\psi$ and $\tau\equiv(t/\varphi)^{3\alpha}$, where φ and ψ are the characteristic time and length scales of the problem. With the power law (24), the dimensional analysis yields

$$\varphi=(c_0/C_3)^{3\alpha/(3\alpha-1)},\quad \psi=\left(c_0^{3\alpha}/C_3\right)^{3\alpha/(3\alpha-1)}, \tag{29}$$

where c_0 is the initial sound speed such that $\psi/\varphi=c_0$, $\psi/C_3\varphi^{3\alpha}=1$. The flow velocity and the sound speed in the (η,τ)-space are then given by $(w,s)=(u,c)/3\alpha C_3t^{3\alpha}$, so the flame moves with a constant speed $w_L=1$, with the flame-front locus and the flow velocity just ahead of it being $\eta_f=\tau$ and $w_f=(\Theta-1)/\Theta$, respectively. The set of partial differential equations of the form (26) and (27) then can be transformed into a set of ordinary differential equations,

$$\frac{dw}{d\xi}=-\left[2\frac{w}{\xi}+\frac{3\alpha-1}{3\alpha}\frac{2}{\gamma-1}+\frac{3\alpha-1}{3\alpha}\frac{w(\xi-w)}{s^2}\right]\times\left[1-\frac{(\xi-w)^2}{s^2}\right]^{-1}, \tag{30}$$

$$\frac{ds^2}{d\xi}=(\gamma-1)\left[(\xi-w)\frac{dw}{d\xi}-\frac{3\alpha-1}{3\alpha}w\right], \tag{31}$$

with the self-similar variable $\xi\equiv\eta/\tau$, and the adiabatic exponent γ. Equations (30) and (31) constitute a scale-invariant problem, with the approximate solution in the (r,t)-space given by

$$\frac{u}{c_0}=3\alpha\left(D_2\frac{\tilde t^{9\alpha-1}}{\tilde r^2}-D_1\frac{\tilde r}{\tilde t}\right), \tag{32}$$

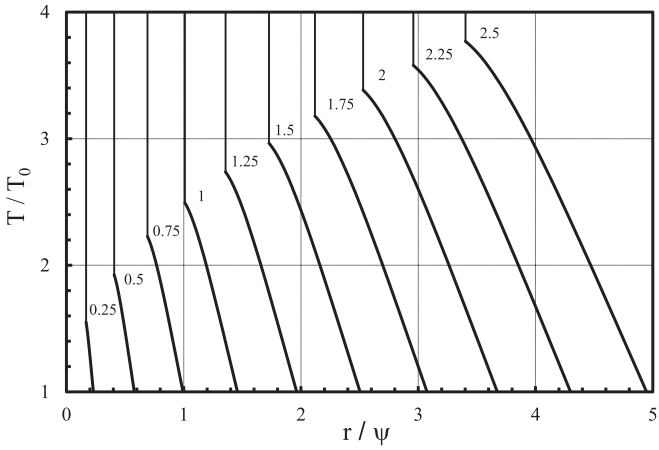

FIG. 4. Scaled temperature profile ahead of the deflagration front for $\Theta=8$, $\gamma=7/5$, and $\alpha=4/3$ at the instants $t/\varphi=0.25\sim2.5$, with the time interval $\Delta t/\varphi=0.25$.

$$T/T_0=1+9\alpha^2(\gamma-1)\left[\left(D_1+\frac{9\alpha-1}{3\alpha}\right)\frac{D_2\tilde t^{9\alpha-2}}{\tilde r}-\frac{D_2^2\tilde t^{18\alpha-2}}{2\tilde r^4}-\left(D_1+\frac{1}{3\alpha}\right)\frac{D\tilde r^2}{2\tilde t^2}-\frac{6\alpha-1}{2\alpha}D_1^{1/3}D_2^{2/3}\tilde t^{6\alpha-2}\right], \tag{33}$$

where $\tilde t=t/\varphi$, $\tilde r=r/\psi$, $T_0\propto c_0^2$ is the room temperature, and

$$D_1=\frac{3\alpha-1}{9\alpha}\frac{2}{\gamma-1},\quad D_2=D_1+\frac{\Theta-1}{\Theta}. \tag{34}$$

The scaled temperature profiles given by Eq. (33) are shown in Fig. 4 for $\Theta=8$, $\gamma=7/5$, and $\alpha=4/3$.

We next consider the trajectories of the unburnt gas parcels upstream of the flame front, described by $u=dr/dt$, with u given by Eq. (32). Specifically, for any given parcel $\{r,t\}$ we can determine the locus $\{r_c,t_c\}$ when this parcel is consumed by the reaction, with $r_c=R_f(t_c)$, unless the parcel explodes earlier by itself and initiates a detonation. We assume, realistically, that the temperature of a gas parcel increases only because of the heat release in the reaction, so the parcel would explode abruptly after an induction time $t_i=t_i\{T(r,t)\}=t_i(r,t)$ [35]. The condition for explosion is then given by [36]

$$t_i(r,t)+t-t_c(r,t)=0. \tag{35}$$

Approximating the temperature dependence of the induction time by a step function $t_i=0$ if $T>T_i$ and $t_i\to\infty$ if $T<T_i$, where T_i is the ignition temperature at which the reaction runs away, similar to Refs. [25,36], we can explore analyticity: the explosion occurs immediately at the flame front as soon as the temperature just ahead of the flame reaches T_i, and the locus of the explosion is given by

$$\tilde t_{\rm expl}/\varphi=\Omega^{1/2(3\alpha-1)},\quad \tilde r_{f,{\rm expl}}/\psi=\Omega^{3\alpha/2(3\alpha-1)}, \tag{36}$$

where

$$\Omega=\frac{(T_i/T_0)-1}{9\alpha^2(\gamma-1)}\left[\left(D_1+\frac{9\alpha-1}{3\alpha}\right)D_2-\frac{D_2^2}{2}-\left(D_1+\frac{1}{3\alpha}\right)\frac{D_1}{2}-\frac{6\alpha-1}{2\alpha}D_1^{1/3}D_2^{2/3}\right]^{-1}. \tag{37}$$

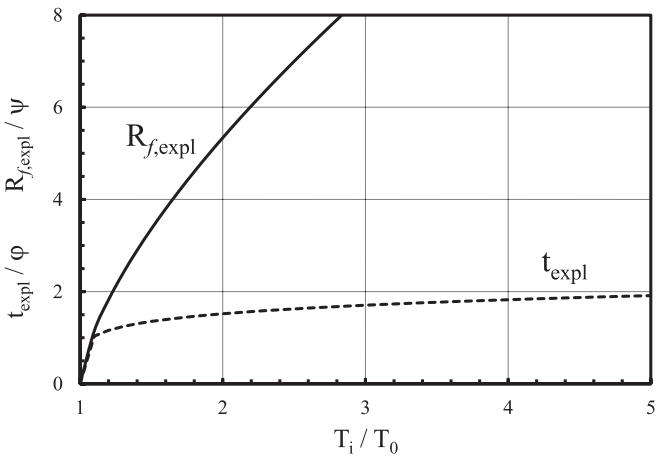

FIG. 5. Scaled instant and position of explosion versus the scaled ignition temperature for $\Theta = 8$, $\gamma = 7/5$, and $\alpha = 4/3$.

The instant and position of explosion given by Eq. (36) are shown in Fig. 5 versus the ignition temperate for $\Theta = 8$, $\gamma = 7/5$, and $\alpha = 4/3$. It is noted that the model of Eqs. (35)–(37) is limited, providing just an estimation, at the hydrodynamic level, for the time and locus of the detonation initiation, while a comprehensive analysis of the diffusive-reactive inner structure of the front and its coupling to the hydrodynamics could quantitatively revise the results.

V. RESULTS AND DISCUSSION

In this study we have presented a formulation describing the dynamics and morphology of outwardly propagating, accelerating turbulent premixed flames and the effect of flame acceleration on explosion triggering. The self-similar nature of the turbulent flame acceleration, given by a well-defined power law based on the average flame radius is determined, and this power-law exponent, Eq. (24), is found to be much larger than that for the hydrodynamically unstable cellular laminar flames, Eq. (19). Hydrodynamic instability is expected to provide additional acceleration at large scales, thus further favoring conditions for detonation triggering. We have also analyzed the dynamics and scalar fields associated with flame propagation, including the time evolution of the flame-generated compression waves, the radial flow velocity, and the trajectories of the fresh gas particles ahead of the flame front, Eq. (32), as well as the evolution of the temperature profile determined by the sound speed in the upstream flow, Eq. (33).

The result (36) is shown in Fig. 4 for $\Theta = 8$, $\gamma = 7/5$, and $\alpha = 4/3$. It is seen that, for a typical $T_i \approx 3T_0$, we have $t_{\rm expl} \approx 10\varphi$ and $R_{f,\rm expl} \approx 25\psi$, and as such the problem is strongly dependent on the time and scale dimensions, φ and ψ. For typical hydrocarbon combustion we find $\varphi \approx (10^{-2} \sim 10^{-1})$s and $\psi \approx (10^{-1} - 10^{0})$m. These values are several orders smaller than those for the freely propagating laminar flames [25], and therefore favor detonation triggering, especially at large spatial dimensions.

While the effect of chamber dynamics is beyond the scope of the present formulation, it is noted that the flame-confinement interaction can influence the acceleration and DDT scenarios. In particular, the acoustic coupling to expanding flames, laminar or turbulent, can modify the power-law flame acceleration, concomitantly facilitating or inhibiting the transition to detonation; see Ref. [37] for details.

Finally, we consider an extension of the above formulation caused by the pressure dependence of the intrinsic flame properties. That is, in later stages of the acceleration, flame-generated compression waves noticeably increase the upstream pressure, thus modifying the unstretched laminar flame speed S_L and the flame thickness δ_L, and thereby the basic characteristics of the flame propagation. An extended self-similar formulation is possible when the second term in the right-hand side of Eq. (33) dominates over unity, with $T \propto t^{6\alpha-2}$, while the isobaric approximation is still valid, $(\Delta P/P)^3 \ll 1$, with $P \propto T^{\gamma/(\gamma-1)} \propto t^{(3\alpha-1)2\gamma/(\gamma-1)}$. Subsequently, with $\lambda_c \propto \delta_L \propto P^{-n/2} \propto t^{-(3\alpha-1)n\gamma/(\gamma-1)}$, and the local mass flow rate $f^0 \propto \Theta S_L \propto P^{(n/2)-1} \propto t^{(n-2)(3\alpha-1)\gamma/(\gamma-1)}$, where n is the global reaction order, Eq. (24) yields

$$R_f \propto (\Theta S_L)^{(9/2)\alpha-3} \lambda_c^{2(1-\alpha)} t^{3\alpha} \propto t^{3\alpha+\{(3\alpha-1)(\alpha-1)2n+(3\alpha-1)(n-2)[(9/2)\alpha-1]\}\gamma/(\gamma-1)}. \quad (38)$$

With $\alpha = 4/3$, $\gamma = 7/5$, Eq. (38) demonstrates a very strong dependence on the reaction order, $R_f \propto t^{4+3.5(17n-30)}$, which can yield either strengthening or weakening correction to Eq. (24) because of compressibility. It is noted that the effect of pressure variations can become of primary importance in astrophysical expanding flames, such as supernovae explosion, which include large pressure gradients in enormous central gravitational field [38].

ACKNOWLEDGMENTS

This work was supported by the Air Force Office of Scientific Research.

[1] R. G. Abdel-Gayed, D. Bradley, and M. Lawes, Proc. R. Soc. London, Ser. A **414**, 389 (1987).
[2] D. Bradley, Proc. Combust. Inst. **24**, 247 (1992).
[3] T. Poinsot and D. Veynante, *Theoretical and Numerical Combustion* (Edwards, Ann Arbor, MI, 2005).
[4] G. Damkohler, Z. Elektrochem. **46**, 601 (1940) [English Translation: NASA Tech. Mem. 1112 (1947)].
[5] N. Peters, *Turbulent Combustion* (Cambridge University Press, New York, 2000).
[6] N. Peters, J. Fluid Mech. **384**, 107 (1999).
[7] S. Chaudhuri, V. Akkerman, and C. K. Law, Phys. Rev. E **84**, 026322 (2011).
[8] V. Akkerman and H. Pitsch, *CTR Annual Research Briefs* (Stanford University, Stanford, CA, 2007), pp. 207–218.
[9] G. Fru, D. Thevenin, and G. Janiga, Energies **4**, 878 (2011).
[10] M. Lawes, M. P. Ormsby, C. G. W. Sheppard, and R. Woolley, Combust. Flame **159**, 1949 (2012).

[11] S. Chaudhuri, F. Wu, D. L. Zhu, and C. K. Law, Phys. Rev. Lett. **108**, 044503 (2012).
[12] F. Wu, G. Jomaas, and C. K. Law, Proc. Combust. Inst. **34**, 937 (2013).
[13] A. Lipatnikov and J. Chomiak, Proc. Combust. Inst. **31**, 1361 (2007).
[14] C. K. Law, *Combustion Physics* (Cambridge University Press, New York, 2006).
[15] V. R. Kuznetsov, Combust., Explos. Shock Waves **18**, 172 (1982).
[16] R. N. Paul and K. N. C. Bray, Proc. Combust. Inst. **26**, 259 (1996).
[17] B. Denet, Phys. Rev. E **55**, 6911 (1997).
[18] B. T. Hellenbrook and C. K. Law, Combust. Flame **117**, 155 (1999).
[19] N. Peters, H. Wenzel, and F. A. Williams, Proc. Combust. Inst. **28**, 235 (2000).
[20] M. Zaytsev and V. Bychkov, Phys. Rev. E **66**, 026310 (2002).
[21] V. Akkerman and V. Bychkov, Combust. Theory Modell. **7**, 767 (2003).
[22] V. Akkerman and V. Bychkov, Combust. Theory Modell. **9**, 323 (2005).
[23] V. Bychkov, A. Petchenko, and V. Akkerman, Combust. Sci. Technol. **179**, 137 (2007).
[24] G. I. Taylor, Proc. R. Soc. London, Ser. A **186**, 273 (1946).
[25] V. Akkerman, C. K. Law, and V. Bychkov, Phys. Rev. E **83**, 026305 (2011).
[26] A. N. Kolmogorov, J. Fluid Mech. **13**, 82 (1962).
[27] S. B. Pope, *Turbulent Flows* (Cambridge University Press, New York, 2000).
[28] Y. Gostintsev, A. Istratov, and Y. Shulenin, Combust., Explos. Shock Waves **24**, 563 (1988).
[29] Y. Gostintsev, Y. Shatskikh, Y. Shulenin, and V. Fortov, Russ. J. Phys. Chem. B **2**, 437 (2008).
[30] D. Bradley, C. G. W. Sheppard, R. Woolley, D. A. Greenhalgh, and R. D. Lockett, Combust. Flame **122**, 195 (2000).
[31] V. V. Bychkov and M. A. Liberman, Phys. Rev. Lett. **76**, 2814 (1996).
[32] G. I. Sivashinsky, Proc. Combust. Inst. **29**, 1737 (2002).
[33] M. A. Liberman, M. F. Ivanov, O. E. Peil, D. M. Valiev, and L.-E. Eriksson, Phys. Fluids **16**, 2476 (2004).
[34] K. L. Pan and R. Fursenko, Phys. Fluids **20**, 094107 (2008).
[35] Ya. B. Zeldovich, G. I. Barenblatt, V. B. Librovich, and G. M. Makhviladze, *Mathematical Theory of Combustion and Explosion* (Consultants Bureau, New York, 1985).
[36] V. Bychkov and V. Akkerman, Phys. Rev. E **73**, 066305 (2006).
[37] V. Akkerman and C. K. Law, Phys. Fluids **25**, 013602 (2013).
[38] V. Akkerman and C. K. Law, Proc. Combust. Inst. **34**, 1921 (2013).